DOI: https://doi.org/10.36094/sc.v89.2024.AC_Impedance_Spectroscopy_Analysis.Ali_Dey.249

ARTICLE

Sci. and Cult. 90 (7–8) : 249-252 (2024)

AC IMPEDANCE SPECTROSCOPY ANALYSIS OF P-Si/$La_{0.7}Sr_{0.3}MnO_3$(LSMO)/CuPc/Au(A) AND P-Si/ $La_{0.7}Sr_{0.3}MnO_3$(LSMO)/P3HT/CuPc/Au(B) HYBRID INORGANIC-ORGANIC HETEROSTRUCTURE UNDER AMBIENT CONDITIONS

MD. MINHAJ ALI[1*] AND P. DEY[1,2*]

Detail AC impedance spectroscopy fitting analysis of p-Si/LSMO/CuPc/Au(A) and p-Si/LSMO/P3HT/CuPc/Au(B) Hybrid Inorganic-Organic heterostructure in ambient conditions has been performed. The real and imaginary part of impedance i.e. Z' and -Z" vs frequency (f) plots for A and B are nearly same in nature. Non-Debye type of relaxation is dominant in both devices. Relaxation peak for B is observed to shift towards lower frequency range than A. Both the devices are fitted well with double circle R(PCR)(PCR) model.

Introduction

Combining Spintronic devices having the advantages of low energy requirements, excellent data manipulation, and memory effect with high speed of light-based technology, developments of cutting edge Opto-Spintronic devices could be possible which have the potential to meet requirements of modern-day advanced information processing. Some important advancement in this direction is Optically Assisted MRAM and All Optical Magnetic Switching which has the potential for efficient data writing in future Opto-Spintronic devices[1]. The quick advancement of research and developments on Organic Spintronic devices including organic spin OLED[2,3], OFET[4], Organic Solar cells and photodetectors[5], etc. lead to the development of the field of Organic Spintronics. Indeed, enhancing the efficiency of power usage in light emitting devices and creating a more affordable, adaptable Organic Opto-spintronic system is very pivotal. Furthermore, Organic Opto-Spintronic devices have the potential to lessen the negative effects of environmental pollution. It is evident from the literature that interfaces between two dissimilar materials play a very crucial role in the performance of any Optoelectronic or Opto-spintronic devices. Apart from that, useful functionalities through the interaction of electrons at the interfaces of hetero-structures, composed of two or more constituent materials with dissimilar properties can be achieved. Additionally, combining synergistically different kinds of functionalities in a heterostructure might lead to creation of new advanced properties that might revolutionise the modern-day information and communication technology. Although a plethora of reports are found in the literature which are vested for understanding the role of these interfaces on spin injection/detection, the knowledge is not conclusive and yet not suitable for device application. In this direction, we have fabricated p-Si/LSMO/CuPc/Au (A) and p-Si/LSMO/P3HT/CuPc/Au (B) Hybrid Inorganic-Organic Hetero structure with an aim to investigate the effect of interfaces on different optoelectronic as well as Opto-Spintronic properties in it. Here, LSMO is a perovskite half metal having spin-dependent band gap and capable of showing spin dependent transport phenomenon, which is renowned for its robustness, is chosen to act as a ferromagnetic

1* Centre for Organic Spintronics and Optoelectronics Devices, Kazi Nazrul University, 713340, Asansol, W.B., India, e-mail: mdminhajali506@gmail.com

2* Department of Physics, Kazi Nazrul University, Asansol, 713340, W.B, India, e-mail:pujaiitkgp2007@gmail.com

spin injector layer[6]. CuPc is an Organic Semiconductor (OSC) that is widely used in photodetectors and solar cells as a holes transportlayer[7, 8]. Similarly, P3HT also acts as a holes transport layer[9]. Finally, owing to its robustness against oxidation Au is chosen to act as an electrode to prevent the degradation of the Organic spacer layer. Here, the holes transport P3HT layer added to achieve the desired improvement in device performance. We get a broadband photo-detection in Visible to IR broad absorption range in B than A, but the magneto-optical coupling effect in B is not better than A, These results will be published in our future communication. Here, in this article, we are focusing only on the AC impedance spectroscopy analysis of A and B, as it is a powerful technique to understand the different interfacial properties happening in Optoelectronic or Opto-Spintronic devices. Here in our device, the overall impedance, real and imaginary parts of impedance in both the samples are found to decrease with an increase in frequency and also observed to meet at nearly the same value at the higher frequency range. The dielectric relaxation peak for B lies in a lower frequency range than A. The Cole-Cole or Nyquist plot for both samples is found to fit well with R(PCR)(PCR) model.

Experimental Details

Thin layer of LSMO has been deposited on p-type Si(100) substrate by Pulsed Laser Deposition technique. CuPc layer of thickness 1200 Å has been deposited on Si/LSMO using thermal evaporation technique and after taking a gap of 10 minutes Gold (Au) is deposited on CuPc layer using e-beam evaporation technique and finally device A is ready. For preparing B, in process of preparing A, an intermediate step of spin coating of P3HT solution with dichlorobenzene having concentration of 5 mg/ml has been performed. The contact is making on the sample using silver paste and 40-gauge copper wire. Data for impedance spectroscopy analysis has been taken with Keysight Impedance Analyzer (E4990A). EIS spectrum analyser software has been used for the fitting analysis of our experimentally taken impedance spectroscopy data[10].

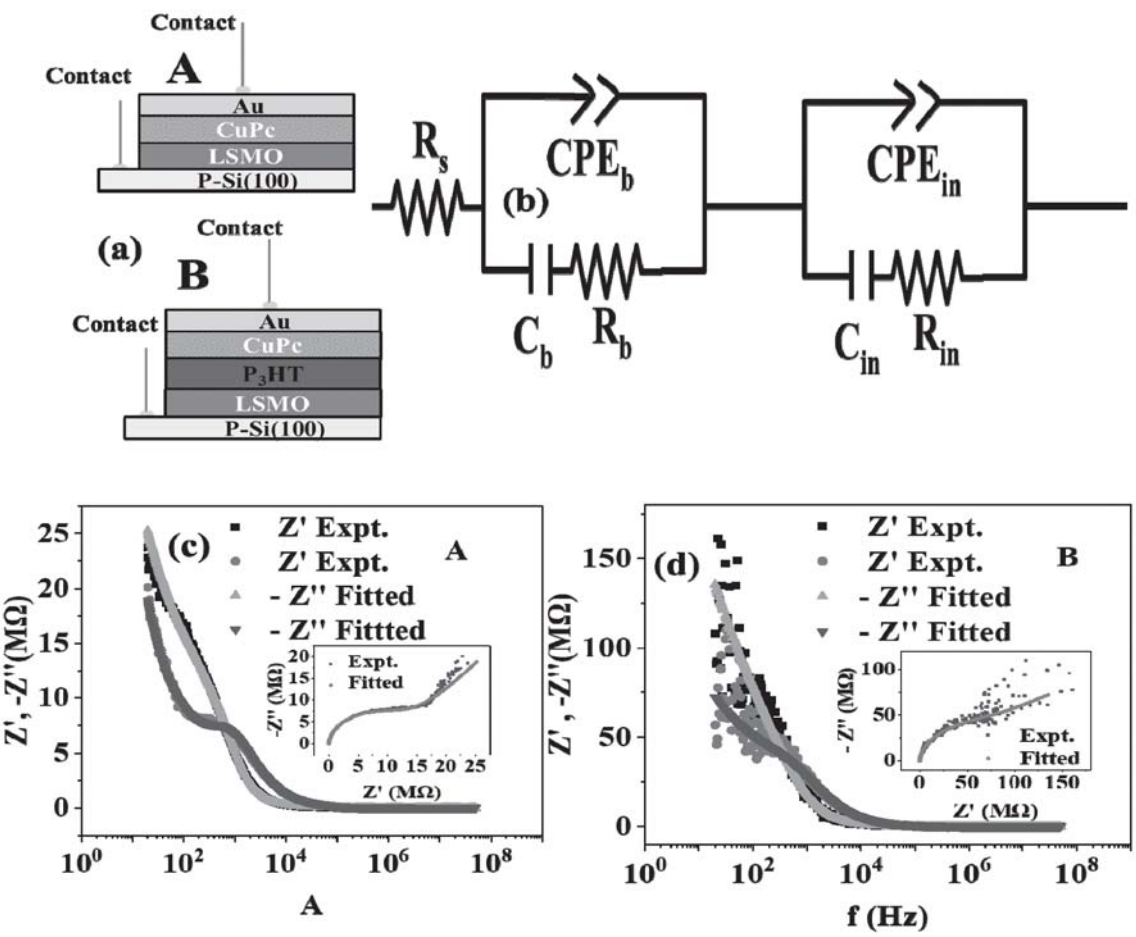

Fig.1. Schematic device structures are shown in (a) for A and B. Equivalent circuit model for fitting analysis is shown in (b). Similarly, Z',-Z'' vs f plots is shown in (c) for A and (d) for B. Insets of (c) & (d) shows corresponding fitting for Nyquist plots.

Results and Discussions

Schematic device structures of A and B are shown in Fig.1.(a). Here, high force end and low force end of impedance analyser is connected to Au and LSMO of both A and B respectively. Fig.1.(b) shows the equivalent model circuit for fitting analysis of impedance spectroscopy data. The magnitude of real and imaginary part of impedance Z',-Z'' vs frequency (f) plots is shown in Fig.1. (c) & (d) for both heterostructure and are observed to decreases with increase in frequency of the AC voltage. Further more, the rapid decrease of Z' and -Z'' value in lower frequency range of 20 Hz to 1000 Hz slows down in the higher frequency side from 1000 Hz to 50 MHz and coincide with each other for both the heterostructure suggest identical conduction mechanism in both hetero structure. We observe a dielectric relaxation peak near about 300 Hz and 550 Hz for A and B suggesting shift in relaxation peak towards lower frequency in B than A.

Table.1. Mathematically calculated result for different circuit parameter for R(PCR)(PCR) model along with error with experimental data for device A and B.

Device-A			Device-B		
Parameter	Result	Error (%)	Parameter	Result	Error (%)
C_b	1.5181E-11	0.87395	C_b	4.0445E-12	7.9754
C_{in}	6.1923E-12	1.4494	C_{in}	3.3671E-12	3.1704
R_s	74.283	10.756	R_s	300.01	5.1452
R_b	54.223	14.737	R_b	303.01	5.0962
R_{in}	461.3	4.197	R_{in}	300.00	5.6094
P_b	4.0912E-08	1.1958	P_b	3.4124E-09	15.447
n_b	0.092811	1.7274	n_b	0.491	2.4509
P_{in}	2.2976E-09	1.2756	P_{in}	2.3874E-09	4.7172
n_{in}	0.64533	0.14366	n_{in}	0.24104	2.508

Furthermore, we obtained best fitted data with our experimental data in R(PCR)(PCR) [Fig.1.(b)] model which is shown in the Fig.1. (c) & (d) as well as in its insets. Here, all the symbols have the conventional meaning and P(CPE) stand for constant phase parameter which is used for non-ideal capacitor elements in a circuit. The truncated and distorted semicircles in both the devices suggest non-Debye type of dielectric relaxation in our device[11,12]. The Nyquist plot for B is slightly noisy in the lower frequency range. The R(PCR)(PCR) model fitted best above frequency range of 100 Hz but it is slightly misfit in very lower frequency range for both A and B. The fitting parameters are shown in the Table.1. Here n is coefficient corresponding to CPE which is used to denote ideal behaviour of CPE. For n = 1, it suggest ideal capacitor. Similarly, R_s, R_b and R_{in} denote the source resistance, OSC bulk resistance of device and charge transfer interface resistance of LSMO/OSC interface. Similarly, C_b, C_{in} denotes OSC bulk capacitance and LSMO/OSC interface capacitance. Additionally, P_b and P_{in} denotes capacitance formed at OSC bulk and different interfaces of LSMO/CuPc, LSMO/P3HT, CuPc/P3HT and CuPc/Au[13]. LSMO/CuPc interface is found to be more efficient in low frequency region that LSMO/P3HT interface from analysis of Nyquist plot and corresponding fitted data which is given in Table.1.

Conclusions

In conclusion, we have fitted our experimental impedance spectroscopy data with R(PCR)(PCR) model and found that our experimental data is best fitted in the frequency range of 100 Hz to 50 MHz. This model is slightly misfit below frequency of 100 Hz. Additionally, our designed model is more accurately fitted with device A than B. Apart from that, Non Debye type of dielectric relaxation process is found to be dominant in both the devices. Furthermore, LSMO/CuPc interface is found to be more efficient in low frequency region than LSMO/P3HT interface. This analysis may be helpful for further understanding of the Optoelectronic and Opto-Spintronic properties of different Inorganic-Organic based hybrid hetero-structures. ❐

References

1. M. Lalieu, R. Lavrijsen, B. Koopmans, *Nat. Commun.,* **10,** 110 (2019).
2. H. Takeno, S. Saito, K. Mizoguchi, *Sci. Rep,* **8,** 15392 (2018).
3. J. P. Prieto-Ruiz, S.G. Miralles, H. Prima-García, A. López-Muñoz, A. Riminucci, P. Graziosi, M. Aeschlimann, M. Cinchetti, V.A. Dediu, E. Coronado, *Adv. Mater.,* **31,**10 (2019).
4. T. Komori, H. Nakanotani,T. Yasuda, C. Adachi,*J. Mater. Chem. C.,* **2,** 4918-4921 (2014).

5. D. Yang. D. Ma, *Adv. Opt. Mater*., **7**, 1800522 (2018).
6. K. Kumari, A. Kumar, D.K. Kotnees, J. Balakrishnan, A. D. Thakur, S.J. Ray,J. Alloys Compd., **815**, 152213 (2020).
7. G. Wei, Z. Lu, Y. Cai, C. Sui, Materials Letters, **201**, 137–139 (2017).
8. D. Nath, P. Dey, A. M. Joseph, J.K. Rakshit, J.N. Roy, *Optical Materials*, **108**, 110371 (2020).
9. Y. Zhang, M. Elawad, Z. Yu, X. Jiang, J. Lai, L. Sun, *RSC Adv*., **6**, 10888-108894 (2016).
10. A.S. Bondarenko, G.A. Ragoisha, Nova Science Publishers: New York, pp. 89–102 (2005).
11. D. Deb, R. Debnath, S. K. Mandal, A. Nath, P. Dey, *J. Alloys Compd*., **776**, 71-82 (2018).
12. H. Ks, G.S. Raju, A.P. Mvn, R. Damle, *J. Appl. Phys*., **118**, 54103 (2015).
13. D. Deb, D. Nath, A. Pal, P. Dey, *Phys. Status Solidi A*, **220**, 2200673 (2023).